Comparison of mean climate trends in the Northern Hemisphere between N.C.E.P. and two Atmosphere-Ocean Model forced runs

Valerio Lucarini

Joint Program on Global Change Science and Policy, MIT, Cambridge, MA 02139 USA

Gary L. Russell

NASA, Goddard Institute for Space Studies, New York, NY 10025 USA

Short title: COMPARISON OF NCEP AND MODEL CLIMATE TRENDS

submitted to: JGR-Atmospheres

Abstract. Results are presented for two greenhouse gas experiments of the Goddard Institute for Space Studies Atmosphere-Ocean Model (AOM). The computed trends of surface pressure, surface temperature, 850, 500 and 200 mb geopotential heights and related temperatures of the model for the time frame 1960-2000 are compared to those obtained from the National Centers for Enviromental Prediction observations. A spatial correlation analysis and mean value comparison are performed, showing good agreement. A brief general discussion about the statistics of trend detection is presented. The domain of interest is the Northern Hemisphere (NH) because of the higher reliability of both the model results and the observations. The accuracy that this AOM has in describing the observed regional and NH climate trends makes it reliable in forecasting future climate changes.

1. Introduction

A complete quantitative comparison of the results of a coupled model with data coming from the observations is needed to test the validity of the model analyzed. In order to assess the credibility of a model to describe climate change, it is necessary to perform a statistical study that analyzes the compatibility of spatial averages and spatial patterns between model and observed trends of climatologically relevant quantities. It is necessary to underline that a major problem that is encountered in such a comparison is the collection of coherent and complete data from observations. In the present report we perform a thorough comparison of the results of two greenhouse gas (GHG) experiments (minus their control simulations) of the Goddard Institute for Space Studies Atmosphere-Ocean Model (AOM) developed by *Russell et al.,* [1995] with climatological data from National Centers for Environmental Prediction (NCEP) reanalysis (see http://www.cdc.noaa.gov/cdc/data.ncep.reanalysis.derived.html) in the time frame 1960-2000. The variables here analyzed are: surface pressure, surface temperature and geopotential height and temperature at 850, 500 and 200 mb.
The surface temperature data of the same model simulations have already been used by *Russell et al.,* [1999] to compare regional changes of surface temperature with the observational data compiled by *Hansen et al.,* [1996, 1999] for the time frame 1960-1998. Therefore we refer to *Russell et al.* for a description of the specific characteristics of the model simulations used. The above mentioned study analyzed two additional runs in which varying tropospheric sulfate aerosols were included in the gr eenhouse gas

experiments. Those experiments have not been considered in this study since they gave poor results in *Russell et al.,*, probably because of a too simplified parametrization of the aerosol effects.

We have decided to perform again the analysis of the surface temperature trend because here it could be inserted in the broader context of a study performed against observational data of different quantities which are all coming from the same source, NCEP. We limit our analysis to the Northern Hemisphere (NH) because the AOM doesn't provide consistent results in the Southern Hemisphere (SH), as already pointed out in *Russell et al.,* [1999], namely Antarctica is warming in one experiment and cooling in another. Another reason for this choice is that there is more confidence in the NCEP data for such a long time frame only in this restricted domain.

2. Procedures

The resolution of the freely available NCEP reanalysis monthly climatological data is 2.5×2.5 degrees. The first procedure is to interpolate those data to the model resolution, which is 4 degrees in latitude × 5 degrees in longitude. We then subtract from the data sets of each of the two GHG experiments the corresponding control data set in order to reduce the effect of climate drift. This reprocessing has been performed in two different ways, the first being through the subtraction from each greenhouse gas experiment of a 21 years moving average of the appropriate control run; the second being through the subtraction of the control run year by year. The two procedures give very similar but not indistinguishable results: results relative to the the 21 years averaging

tecnique as in *Russell et al.,* [1999] are presented here because they are conceptually closer to the idea of climate drift subtraction. We thus obtain for each climatological variable the two model data sets GHG1 and GHG2. In order to reduce the influence of model noise through averaging GHG1 and GHG2, a new data set for all variables is created and named GHGs.

At every grid cell and for every variable previously described, the trend is computed as the slope of the least square fit line of the seasonal and annual values for the years 1960 to 2000. Then, for each of these variables, the spatial correlations between the NH trends of NCEP vs. GHG1, NCEP vs. GHG2, NCEP vs. GHGs and GHG1 vs. GHG2 are computed (see *Johns et al.,* 2001 for another spatial correlation analysis of modeled and observed surface temperature trends). The last two correlations are the most relevant ones because GHGs contains the statistically most significant information we can deduce from the models runs, while comparing GHG1 vs. GHG2 gives us an estimate of the model self-consistency and stability. The presence of small or negative spatial correlations between GHG1 and GHG2 data sets in the SH has forced us to limit the study to the NH. In all grid cells where the 850 mb geopotential height has crossed the surface at least once in the 41 year record, the 850 mb data has been discarded from all analyses. These grid cells are blank on the GHGs 850 mb geopotential height and temperature plates. The NCEP 850 mb NH mean trends were computed both considering and excluding these grid cells.

For the NCEP and GHGs data sets the trend of the NH spatial mean and its 0.95 confidence interval are computed for each of the variables considered following the

procedure described by *Weatherhead et al.,* [1998]. To compute the annual mean trend. it assumed a linear trend model of the form $Y_s = \mu + \omega X_s + S_s + N_s$ where s is the season index (it runs from 1 to 164 = 4×41 years), Y_s is the actual NH spatial mean, μ is a constant term, $X_s = s/4$ is the linear trend function, ω is the magnitude of the trend per year, S_s is the seasonal oscillating term which is identical every fourth season, and N_s is the noise. We assume N_s to be an AR(1) noise, that is the following relation holds: $N_s = \phi N_{s-1} + \epsilon_s$, where $\phi = Corr(N_s, N_{s-1})$ and ϵ_s is random uncorrelated noise Weatherhead et al. The seasonal term S_s is subtracted from the data set to simplify the linear trend model as $Y_s = \mu + \omega X_s + N_s$; minimizing the residual the best estimates $\bar{\mu}$ and $\bar{\omega}$ are obtained. In *Weatherhead et al.* an exact but rather cumbersome formula for the variance of the trend ω is given in the Appendix; this formula (not reported here) is used to compute the 0.95 confidence intervals. It should be observed that if m is the number of records per year (four in this case, twelve in *Weatherhead et al.*) the approximate formula for the variance of ω presented in eq.(2) of *Weatherhead et al.* should be multiplied by a factor $(6/m)^{1/2}$ to make it consistent with the exact derivation presented in the Appendix. To compute the seasonal NH mean trend confidence intervals we follow the same procedure: in this case there is only one record per year (the season considered) and obviously the term S is not present.

It should be stressed that the procedure of using all the seasonal value instead of the annual average in order to compute the annual trend reduces the 0.95 confidence interval of such a trend (essentially having the same mean value), the fundamental reason being that more information is retrieved (there are $4 \times n$ data instead of n, if n is

the number of years available). An important consequence is to have smaller confidence intervals for the annual trends than for the seasonal ones. This facts can be particularly important for those data sets, like those of the Microwave Sounding Unit (MSU), which have such a short time length that trends can be hardly recognized. Applying this procedure to well known data, like that in *Angell,* [1999] it is possible to obtain better constrained statistics (Lucarini, unpublished results, 2001) than those published. To assess the overall validity of the NCEP NH mean trends, a preliminary comparison of NCEP data and radiosonde data [*Angell,* 2000] for the NH mean surface temperature and 850-300 mb layer virtual temperature trends for the time frame 1958-1999 was performed, showing good agreement between the two data sets. The obtained 0.95 confidence intervals overlap for both variables, in particular for the annual trends. This overall correspondence between these two data sets agrees with the conclusions drawn by *Trenberth et al.,* [1998] on this subject for the tropical region. A detailed comparison of NCEP reanalysis data, Angell radiosonde data and MSU data will be presented elsewhere (Lucarini, unpublished results, 2001) .

3. Results

Tables 1-3 present the NH spatial correlation analysis for temperature, surface pressure and geopotential height respectively. Tables 4-6 present NH mean trends and their 0.95 confidence intervals for the same quantities. Plates 1-8 give a portrait of the spatial patterns of GHGs and NCEP winter (DJF) and annual (ANN) average trends of the variables analyzed. For all variables considered, the highest correlations

Tables 1-3

Tables 4-6

Plates 1-8

between NCEP data and model experiments occur in winter and spring, while the worst comparison occur in summer. This can be explained by the fact that the model has deficiencies in some aspects of climate that play a more relevant role in summer, like cloud feedback and the hydrological cycle. In addition, summer data are more noisy, as can be seen from the fact that the confidence intervals of the mean trends are much wider in summer for all variables for both GHGs and NCEP data sets. The spatial correlation of the annual means is usually fairly good and resembles the corresponding winter correlation, thanks to the fact that the winter signal has usually the strongest local features and at the same time has the least noise. It should be observed that for every variable the spatial correlation between the two model experiments are smaller than those between each of them and NCEP data. This suggests that the natural variability of the model is larger than the observed one. Another general characteristic of the results presented is that the GHGs trends usually underestimate the local maxima and minima compared to NCEP. This is partly beacause GHGs is an average of two experiments while NCEP is a single realization. Another possible explanation of this can be found in the fact [Shindell et al., 1999] that this model presents an AO index trend which is about one third of the observed value, thus having a smaller increase of the average intersity of western winds over the Atlantic Ocean. Since the presence of an AO index trend essentially creates a zonal redistribution of heat, its underestimation shouldn't dramatically effect the reliability of mean hemispheric trends. It is interesting to note that the model data presents higher values than the NCEP data for the spatial correlation coefficient between the seasonal and annual trends of surface temperature

and temperature at 850 mb, the former ranging around 0.8-0.9, the latter around 0.4-0.7. The NH mean trend confidence intervals match well for all variables for both seasonal trends and the annual trend, with the interesting exception of surface pressure. The width of the confidence intervals determined from the GHGs data is usually smaller than those deduced from NCEP data; the latter ones become larger than the former ones as we look higher in the atmosphere, where NCEP data seem very noisy. It is important to stress that the small width of the confidence intervals of the trends deduced from the GHGs data sets are related to the procedure through which these data sets were created; a GHGs confidence interval should generally be smaller than either the GHG1 or GHG2 confidence interval itself. We observe that, coherently with the theory presented in the previous section, the confidence interval for the annual trends is always smaller than those of the seasonal trends.

We now present, variable by variable, some comments about the spatial correlations and the NH mean trends obtained from NCEP and GHGs data sets.

Surface temperature (Plate 1): The main disagreement between the two trend maps is that in the GHGs data Greenland, western USA and southern Asia are not cooling and cooling in the Sahara desert and heating in central Siberia are underestimated. The spatial pattern between the model and NCEP match well over the oceans, with warming over the Arctic Ocean and cooling over the North Atlantic [*Russell and Rind,* 1999] and North Pacific Oceans. The overall effect of the disagreement is the presence of slightly higher mean trends for the GHGs data, although the confidence interval still show overlapping.

Temperature at 850 mb (Plate 2): The model results agree with NCEP in the western portion of the hemisphere, while the patterns don't match in the eastern portion, particularly for the annual trend. Except for winter and spring the spatial correlation coeffcient between the model and NCEP are negative. The 850 mb temperature over the Arctic Ocean is warming in the model (as it is at the surface), whereas NCEP shows a small trend on the annual average. On the contrary, the hemispheric mean trends match very well for all seasons and for the annual trends, presenting strongly overlapping confidence levels.

Temperature at 500 mb (Plate 3): The agreement over the north-western quarter sphere is excellent, whereas the model misses some NCEP extremes and is too hot in the north-east, so that a large bias between the NCEP and GHGs hemispheric mean trends exists.

Temperature at 200 mb (Plate 4): The NCEP and GHGs trend patterns are similar, presenting a northward decrease over the Arctic Ocean of the trends which is opposite to that which occurs at the surface. The NCEP data show a very deep minimum over the Arctic Ocean whose intensity is not captured by GHGs data. This causes a large difference between the NH mean trends except in winter: the model is always too hot.

Surface pressure (Plate 5): The model captures the spatial patterns of the NCEP observations. In particular there is a signal of an increase in the AO index over time [Shindell et al., 1999]. This quantity has the best spatial correlation of all, but the hemispheric mean trend of the model is negligeable and totally not compatible with the NCEP one, that is strongly positive, the main cause being an underestimation of the

positive trends over Europe and Central-Southern Asia. The model's surface pressure is the dry atmopsheric pressure which is constant globally. The model does indicate an increase of global surface pressure of about .02 mb/decade due to the increase of humidity between 1960 and 2000. The NCEP data indicate a more significant shift of mass from the SH into the NH.

Geopotential height at 850 mb (Plate 6): The model and NCEP compare favorably over the Oceans and North America but are poorly correlated over Asia. The model's mean trends are considerably weaker than those of NCEP, and, based on the confidence intervals, they barely overlap or even do not.

Geopotential height at 500 mb (Plate 7): The patterns in the western part of the NH present good agreement in winter and in the annual averages, while the GHGs trends in the eastern part are poorly correlated with NCEP's. The model underestimates the mean trends, because it underestimates the maxima more seriously. In any case the confidence intervals overlap, barely.

Geopotential height at 200 mb (Plate 8): The latitudinal average of the spatial patterns match well while some of the longitudinal features show differences between the model and NCEP. The NCEP data feature deeper minima and higher maxima. As seen for the 200 mb temperature, the NCEP confidence intervals are much greater than those of model which indicate a much greater interannual variability of 200 mb quantities.

4. Conclusions

A thorough comparison between NCEP reanalysis data and two GISS AOM greenhouse gases forced runs have been performed in order to assess the credibility of this model to describe regional and NH mean trends for several climatologically relevant variables: surface pressure and temperature and geopotential height and temperature at 850, 500 and 200 mb. A spatial correlation analysis has been performed with very positive results for the winter data and the annual trends for all the variables considered. The NH mean trends together with their 0.95 confidence intervals have been computed, showing for all variables except surface pressure a good agreement between the NCEP and GISS AOM outputs in terms of statistical significance for most seasonal and annual trends. Computing the annual trends using all the seasonal data instead of the annual average is statistically more efficient because more infromation is retrieved, thus restricting the confidence intervals. The GISS AOGCM has been able to capture the climatological evolution of the last forty years with remarkable accuracy in describing both local features and NH average trends, and therefore can be considered reliable for future projections. This study more generally stresses the importance of using mathematical tools able to capture the compatibility of both regional and global results of trends deduced from a model and observations in order to assess more rigorously a model's reliability and efficacy in forecasting future climate change. More information and quantities for these AOM simulations are available at: http://aom.giss.nasa.gov.

Acknowledgments. We are grateful to D. Rind for useful suggestions. One author

(V.L.) would like to thank G. Schmidt, D. Rind and R. Miller for stimulating conversations and all of GISS for the warm hospitality received while visiting during Summer 2001.

References

J.K. Angell, Global, hemispheric, and zonal temperature deviations derived from radiosonde records. In Trends Online: A Compendium of Data on Global Change. Carbon Dioxide Information Analysis Center, Oak Ridge National Laboratory, U.S. Department of Energy, Oak Ridge, Tennessee, U.S.A. (data available at: http://cdiac.esd.ornl.gov/trends/temp/angell/angell.html)

J.E. Hansen, R. Ruedy and M. Sato, Global Surface air temperature in 1995: Return to pre-Pinatubo level, *Geophys. Res. Lett., 23,*, 1665-1668, 1996.

J.E. Hansen, R. Ruedy, J. Glascoe and M. Sato, GISS analysis of surface temperature change, *J. Geophys. Res., 104*, 30997-31022, 1999.

G.L. Russell, J.R. Miller and D. Rind, A coupled atmosphere-ocean model for transient climate change studies,*Atmos. Ocean, 33(4)*, 683-730, 1995.

G.L. Russell, J.R. Miller, D. Rind, R. A. Ruedy, G.A. Schmidt, S. Sheth, Comparison of model and observed regional temperature changes during the last 40 years. *J. Geophys. Res., 105* 14891-14898, 1999.

G.L. Russell and D. Rind, Response to CO2 transient increase in the GISS coupled model: regional coolings in a warming climate, *J. Clim., 12*, 531-539, 1999.

D. T. Shindell, R.L. Miller, G.A. Schmidt and L. Pandolfo, Simulations of recent northern winter climate trends by greenhouse gas forcing,*Nature, 339*, 569-572, 1999.

J.K. Angell, Comparison of surface and tropospheric temperature trends estimated from a 63-station radiosonde network, 1958-1998, *Geophys. Res. Lett., 25*, 2761-2764, 1999.

E.C. Weatherhead, G.C. Reinsel, G.C. Tiao, X.L. Meng, D. Choi, W.K. Cheang, T. Keller, J. DeLuisi, D.J. Wuebbles, J.B. Kerr, A.J. Miller, S.J. Oltmans and J.E. Frederick,

Factors affecting the detection of trends: Statistical considerations and applications to environmental data, *J. Geophys. Res., 103*, 17149-17161, 1998.

K.E. Trenberth, D.P. Stepaniak, J.W. Hurrell and M.Fiorino, Quality of Reanalyses in the Tropics, *J. Clim., 14*, 1499-1510, 2001.

T.C. Johns, J.M. Gregory, P.A. Stott and J.F.B Mitchell, Correlations between patterns of 19th and 20th century surface temperature change and HadCM2 climate model ensembles. *Geophys. Res. Lett.,* , *28*, 1007-1010.

Valerio Lucarini, Joint Program on Global Change Science and Policy, MIT, Cambridge, MA 02139, USA (e-mail: lucarini@mit.edu)

Gary L. Russell, NASA, Goddard Institute for Space Studies, New York, NY 10025, USA (e-mail: grussell@giss.nasa.gov)

Received _____

Plate 1. Spatial patterns of the NCEP and GHGs winter (DJF) and annual (ANN) average trends of surface temperature

Plate 2. Spatial patterns of the NCEP and GHGs winter (DJF) and annual (ANN) average trends of temperature at 850 mb

Plate 3. Spatial patterns of the NCEP and GHGs winter (DJF) and annual (ANN) average trends of temperature at 500mb

Plate 4. Spatial patterns of the NCEP and GHGs winter (DJF) and annual (ANN) average trends of temperature at 200mb

Plate 5. Spatial patterns of the NCEP and GHGs winter (DJF) and annual (ANN) average trends of surface pressure

Plate 6. Spatial patterns of the NCEP and GHGs winter (DJF) and annual (ANN) average trends of geopotential height at 850 mb

Plate 7. Spatial patterns of the NCEP and GHGs winter (DJF) and annual (ANN) average trends of geopotential height at 500 mb

Plate 8. Spatial patterns of the NCEP and GHGs winter (DJF) and annual (ANN) average trends of geopotential height at 200 mb

Table 1. Spatial correlation coefficients of temperature trends from NCEP and GHG experiments for the Northern Hemisphere

		DJF	MAM	JJA	SON	ANN
TAS	NCEP vs. GHGs	0.585	0.690	0.076	0.693	0.648
	NCEP vs. GHG1	0.568	0.461	-0.006	0.658	0.528
	NCEP vs. GHG2	0.484	0.659	0.113	0.588	0.561
	GHG1 vs. GHG2	0.537	0.382	-0.054	0.601	0.408
T850	NCEP vs. GHGs	0.393	0.174	-0.221	-0.289	-0.083
	NCEP vs. GHG1	0.541	0.165	-0.295	-0.308	0.081
	NCEP vs. GHG2	0.090	0.110	0.005	-0.161	-0.182
	GHG1 vs. GHG2	0.173	0.204	-0.050	0.295	0.110
T500	NCEP vs. GHGs	0.560	0.458	0.062	0.290	0.390
	NCEP vs. GHG1	0.533	0.269	0.038	0.193	0.360
	NCEP vs. GHG2	0.308	0.372	0.064	0.267	0.134
	GHG1 vs. GHG2	0.135	-0.033	0.291	0.246	-0.155
T200	NCEP vs. GHGs	0.455	0.413	0.218	0.379	0.502

Table 1. (continued)

	DJF	MAM	JJA	SON	ANN
NCEP vs. GHG1	0.313	0.314	0.185	0.347	0.456
NCEP vs. GHG2	0.453	0.413	0.205	0.345	0.459
GHG1 vs. GHG2	0.363	0.484	0.584	0.651	0.658

Table 2. Spatial correlation coefficients of surface pressure trends from NCEP and GHG experiments for the Northern Hemisphere

		DJF	MAM	JJA	SON	ANN
SURPRES	NCEP vs. GHGs	0.815	0.669	0.148	0.211	0.654
	NCEP vs. GHG1	0.713	0.419	0.027	-0.058	0.487
	NCEP vs. GHG2	0.585	0.394	0.233	0.316	0.464
	GHG1 vs. GHG2	0.289	-0.292	0.339	-0.254	0.024

Table 3. Spatial correlation coefficients of geopotential height trends from NCEP and GHG experiments for the Northern Hemisphere

		DJF	MAM	JJA	SON	ANN
Z850	NCEP vs. GHGs	0.746	0.573	0.114	0.198	0.474
	NCEP vs. GHG1	0.670	0.371	0.020	-0.172	0.353
	NCEP vs. GHG2	0.456	0.328	0.175	0.369	0.240
	GHG1 vs. GHG2	0.173	-0.257	0.209	-0.083	-0.200
Z500	NCEP vs. GHGs	0.701	0.521	0.054	0.024	0.372
	NCEP vs. GHG1	0.677	0.341	-0.078	-0.237	0.385
	NCEP vs. GHG2	0.345	0.337	0.180	0.216	0.053
	GHG1 vs. GHG2	0.110	-0.153	0.111	0.224	-0.246
Z200	NCEP vs. GHGs	0.794	0.552	0.101	-0.046	0.620
	NCEP vs. GHG1	0.815	0.409	0.097	-0.083	0.584
	NCEP vs. GHG2	0.387	0.232	0.058	0.011	0.056
	GHG1 vs. GHG2	0.209	-0.317	0.261	0.031	-0.364

Table 4. Trends of the NCEP and GHGs N.H. mean temperatures and related 0.95 confidence intervals (in K/decade)

			DJF	MAM	JJA	SON	ANN
TAS	GHGs	TREND	0.17	0.16	0.11	0.17	0.16
		C.I.	0.03	0.05	0.03	0.03	0.02
	NCEP	TREND	0.12	0.14	0.11	0.11	0.12
		C.I.	0.07	0.05	0.04	0.06	0.04
T850	GHGs	TREND	0.14	0.15	0.13	0.17	0.15
		C.I.	0.02	0.04	0.03	0.02	0.02
	NCEP[a]	TREND	0.14 (0.15)	0.20 (0.22)	0.18 (0.19)	0.16 (0.17)	0.17 (0.18)
		C.I.	0.08 (0.08)	0.06 (0.06)	0.05 (0.05)	0.07 (0.08)	0.03 (0.03)
T500	GHGs	TREND	0.12	0.15	0.18	0.18	0.16
		C.I.	0.02	0.04	0.05	0.02	0.02
	NCEP	TREND	0.07	0.04	0.05	0.08	0.06
		C.I.	0.08	0.06	0.07	0.07	0.04
T200	GHGs	TREND	0.12	0.13	0.19	0.19	0.16

Table 4. (continued)

		DJF	MAM	JJA	SON	ANN
	C.I.	0.03	0.05	0.04	0.03	0.02
NCEP	TREND	0.14	0.05	0.05	0.11	0.09
	C.I.	0.11	0.15	0.16	0.14	0.08

[a]The quantities between paratheses have been computed excluding the grid cells where T850 is not defined in the model

Table 5. Trends of the NCEP and GHGs N.H. mean surface pressure and related 0.95 confidence intervals (in mb/decade)

			DJF	MAM	JJA	SON	ANN
SURPRES	GHGs	TREND	0.00	-0.01	-0.01	-0.03	-0.01
		C.I.	0.05	0.03	0.04	0.04	0.03
	NCEP	TREND	0.06	0.12	0.23	0.18	0.15
		C.I.	0.07	0.06	0.10	0.10	0.04

Table 6. Trends of the NCEP and GHGs N.H. mean geopotential heights and related 0.95 confidence intervals (in m/decade)

			DJF	MAM	JJA	SON	ANN
Z850	GHGs	TREND	0.7	0.6	0.5	0.4	0.6
		C.I.	0.4	0.3	0.3	0.4	0.2
	NCEP[a]	TREND	1.3 (1.2)	2.0 (1.8)	3.0 (2.7)	2.4 (2.2)	2.2 (2.0)
		C.I.	0.7 (0.7)	0.6 (0.6)	1.1 (1.2)	0.9 (1.0)	0.5 (0.5)
Z500	GHGs	TREND	2.6	2.9	2.9	3.2	2.9
		C.I.	0.4	0.9	0.5	0.5	0.3
	NCEP	TREND	3.1	3.6	4.5	4.1	3.9
		C.I.	1.8	1.2	1.7	1.2	0.9
Z200	GHGs	TREND	6.2	6.9	8.4	8.6	7.7
		C.I.	0.8	2.0	1.6	1.0	0.8
	NCEP	TREND	6.1	5.1	6.6	7.2	6.2
		C.I.	4.6	3.6	4.4	3.8	2.2

[a]The quantities between paratheses have been computed excluding the grid cells where Z850 is not defined in the model

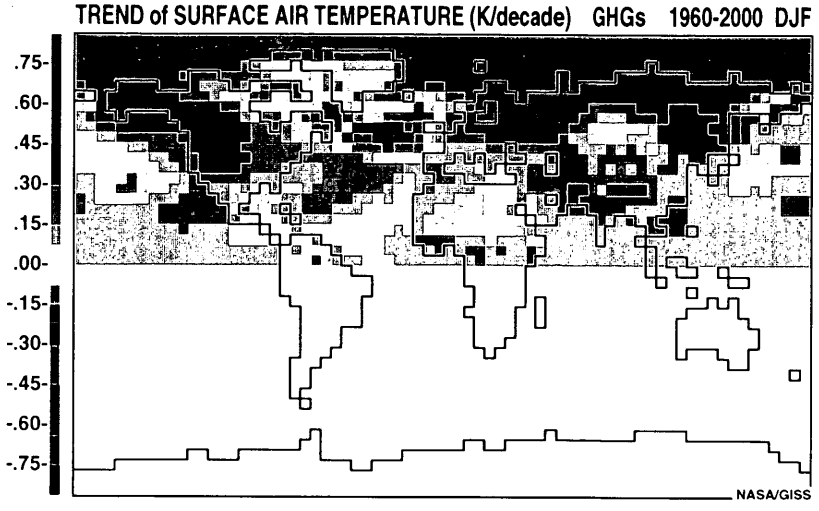
TREND of SURFACE AIR TEMPERATURE (K/decade) GHGs 1960-2000 DJF
.75
.60
.45
.30
.15
.00
-.15
-.30
-.45
-.60
-.75
NASA/GISS

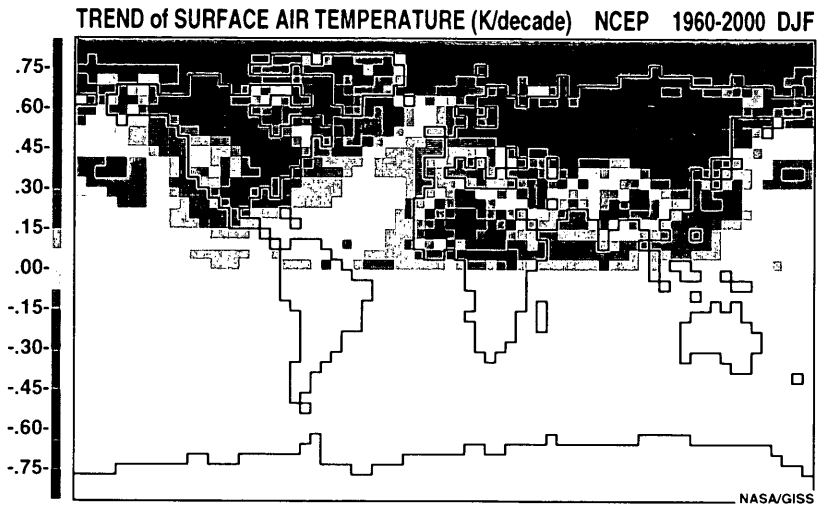
TREND of SURFACE AIR TEMPERATURE (K/decade) NCEP 1960-2000 DJF
.75
.60
.45
.30
.15
.00
-.15
-.30
-.45
-.60
-.75
NASA/GISS

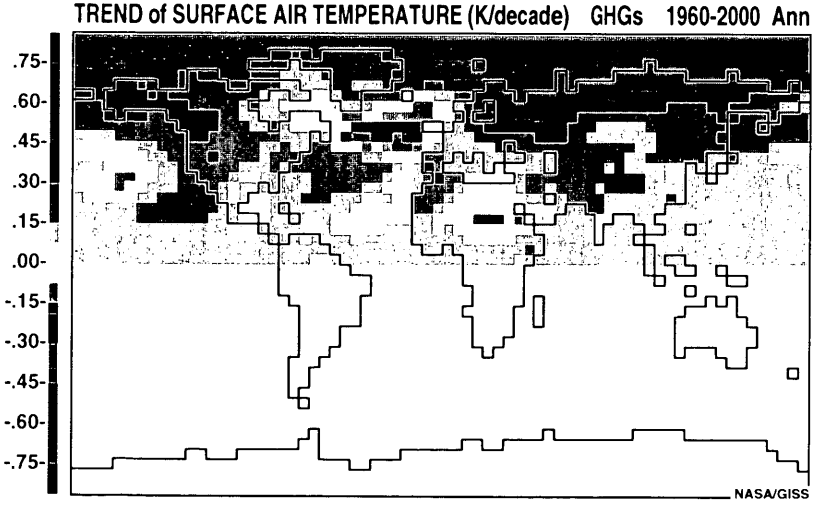
TREND of SURFACE AIR TEMPERATURE (K/decade) GHGs 1960-2000 Ann
.75
.60
.45
.30
.15
.00
-.15
-.30
-.45
-.60
-.75
NASA/GISS

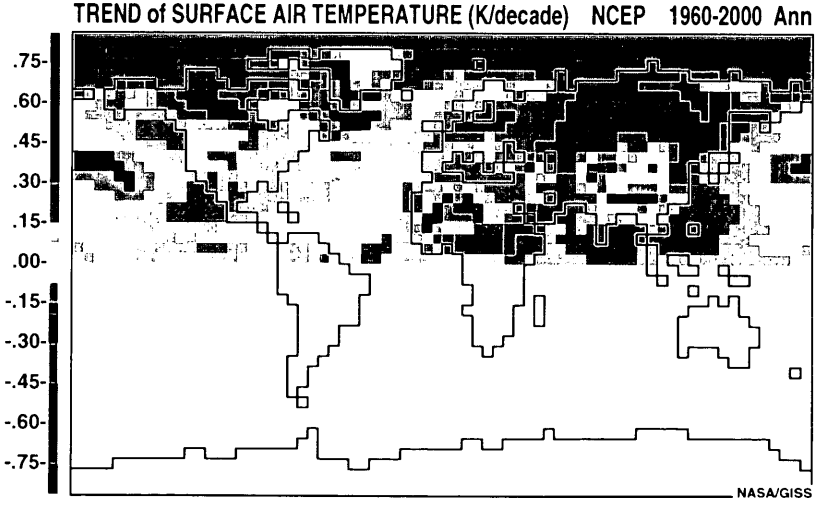
TREND of SURFACE AIR TEMPERATURE (K/decade) NCEP 1960-2000 Ann
.75
.60
.45
.30
.15
.00
-.15
-.30
-.45
-.60
-.75
NASA/GISS

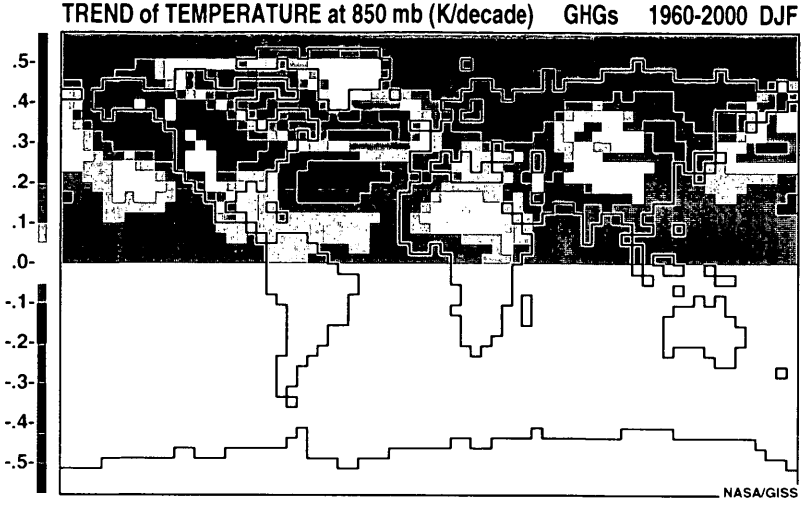
TREND of TEMPERATURE at 850 mb (K/decade) GHGs 1960-2000 DJF
.5
.4
.3
.2
.1
.0
-.1
-.2
-.3
-.4
-.5
NASA/GISS

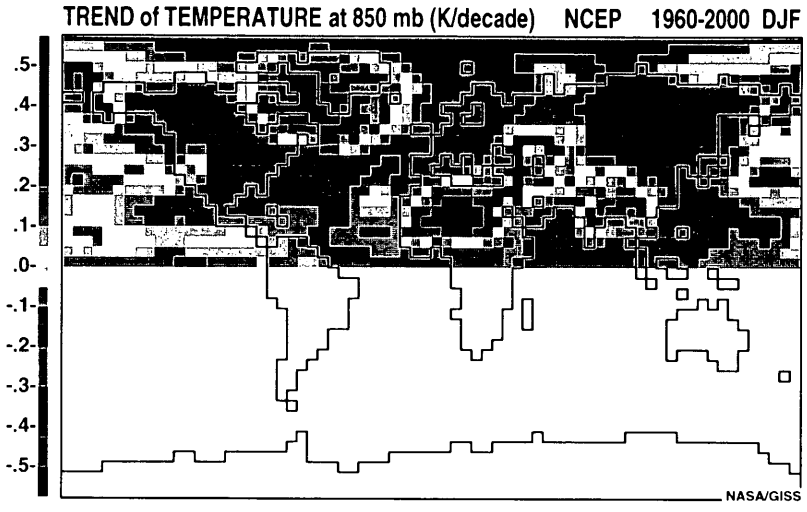
TREND of TEMPERATURE at 850 mb (K/decade) NCEP 1960-2000 DJF
.5
.4
.3
.2
.1
.0
-.1
-.2
-.3
-.4
-.5
NASA/GISS

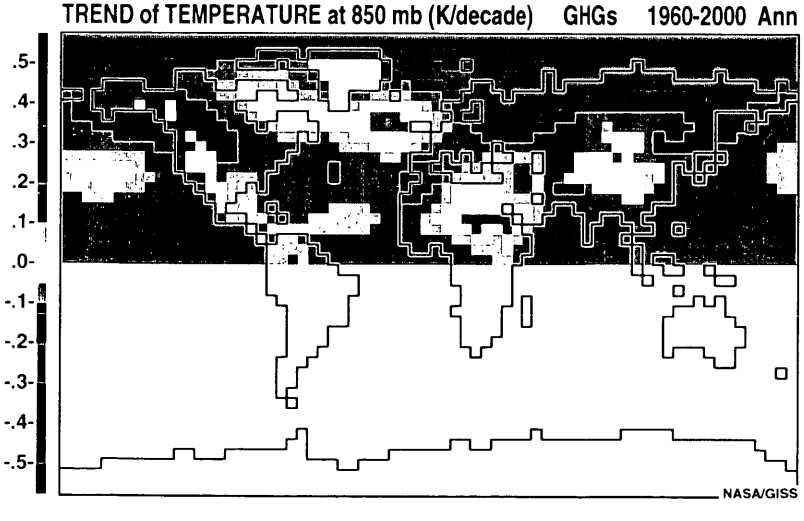
TREND of TEMPERATURE at 850 mb (K/decade) GHGs 1960-2000 Ann
.5
.4
.3
.2
.1
.0
-.1
-.2
-.3
-.4
-.5
NASA/GISS

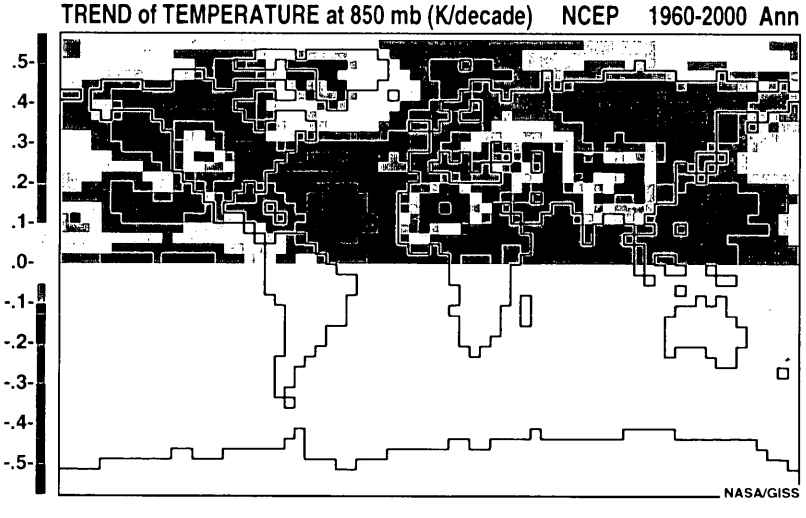
TREND of TEMPERATURE at 850 mb (K/decade) NCEP 1960-2000 Ann
.5
.4
.3
.2
.1
.0
-.1
-.2
-.3
-.4
-.5
NASA/GISS

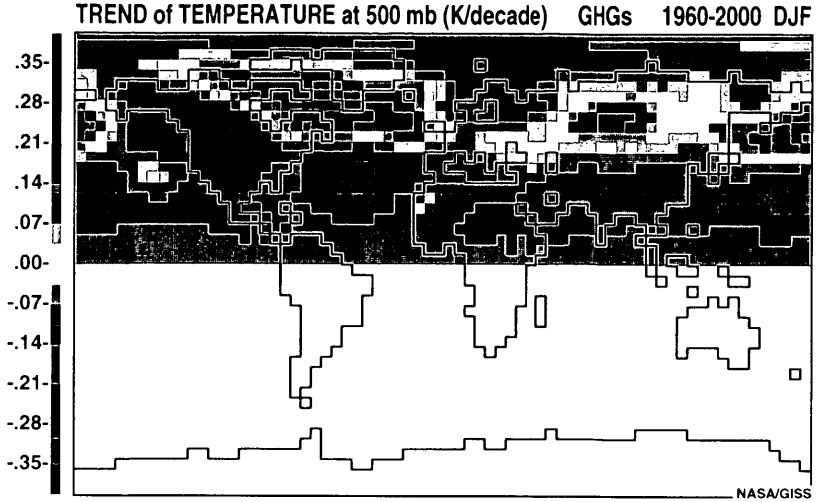
TREND of TEMPERATURE at 500 mb (K/decade) GHGs 1960-2000 DJF
.35-
.28-
.21-
.14-
.07-
.00-
-.07-
-.14-
-.21-
-.28-
-.35-
NASA/GISS

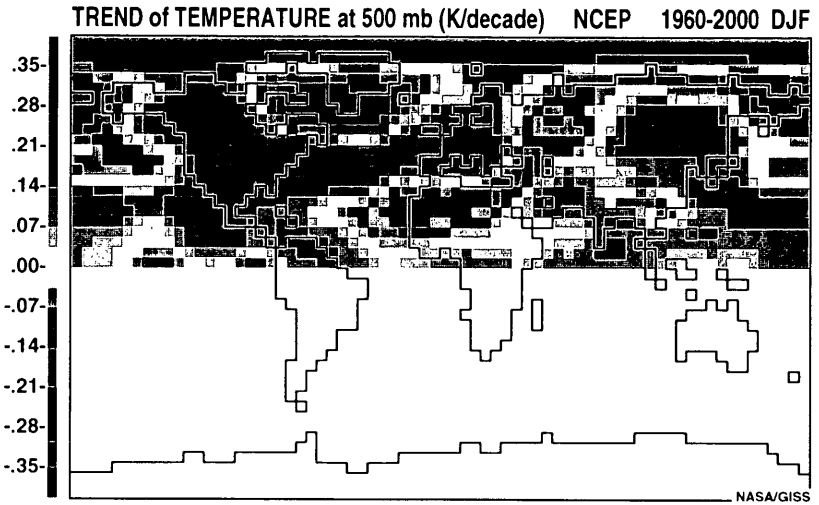
TREND of TEMPERATURE at 500 mb (K/decade) NCEP 1960-2000 DJF
.35-
.28-
.21-
.14-
.07-
.00-
-.07-
-.14-
-.21-
-.28-
-.35-
NASA/GISS

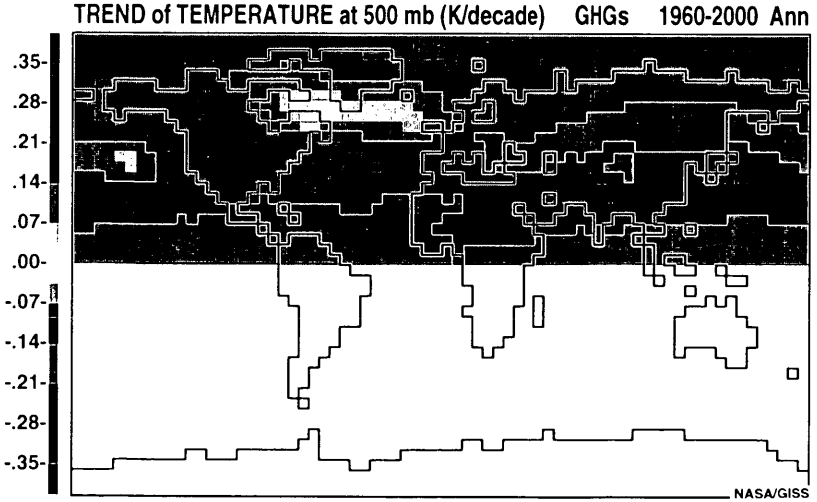
TREND of TEMPERATURE at 500 mb (K/decade) GHGs 1960-2000 Ann
.35-
.28-
.21-
.14-
.07-
.00-
-.07-
-.14-
-.21-
-.28-
-.35-
NASA/GISS

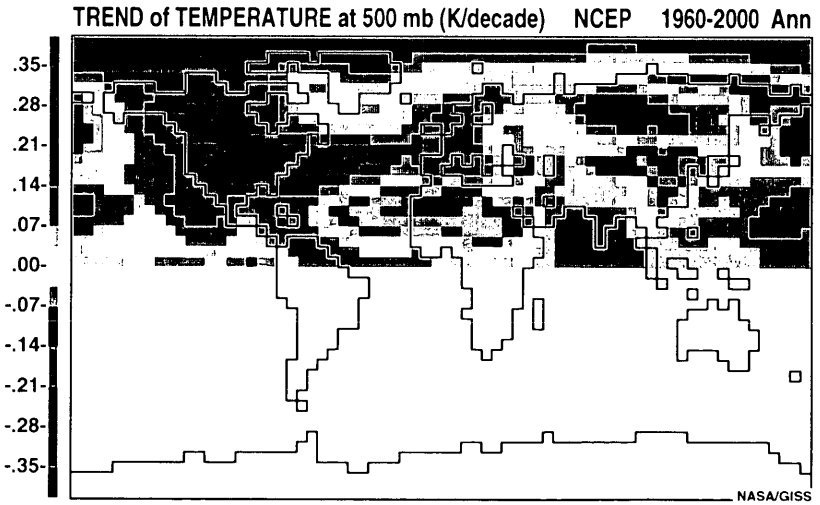
TREND of TEMPERATURE at 500 mb (K/decade) NCEP 1960-2000 Ann
.35-
.28-
.21-
.14-
.07-
.00-
-.07-
-.14-
-.21-
-.28-
-.35-
NASA/GISS

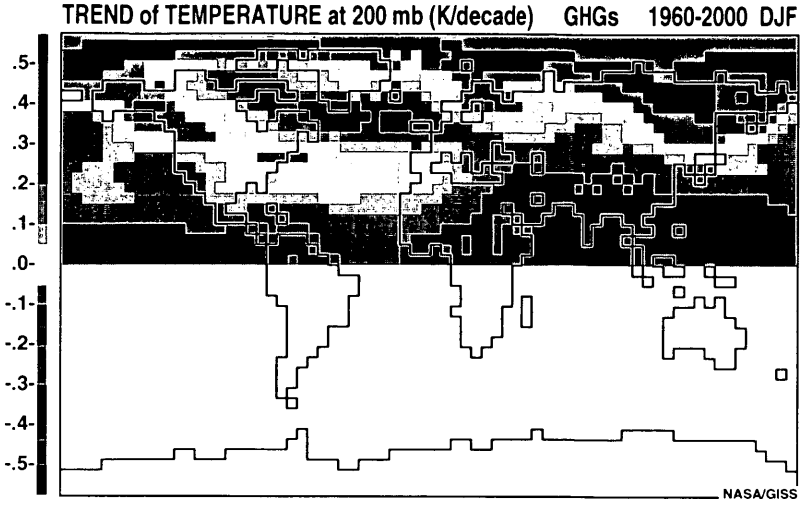
TREND of TEMPERATURE at 200 mb (K/decade) GHGs 1960-2000 DJF
.5-
.4-
.3-
.2-
.1-
.0-
-.1-
-.2-
-.3-
-.4-
-.5-
NASA/GISS

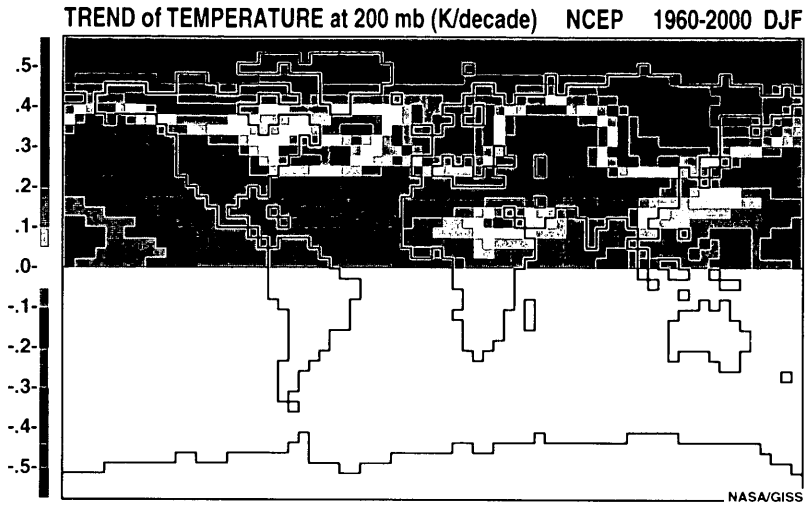
TREND of TEMPERATURE at 200 mb (K/decade) NCEP 1960-2000 DJF
.5-
.4-
.3-
.2-
.1-
.0-
-.1-
-.2-
-.3-
-.4-
-.5-
NASA/GISS

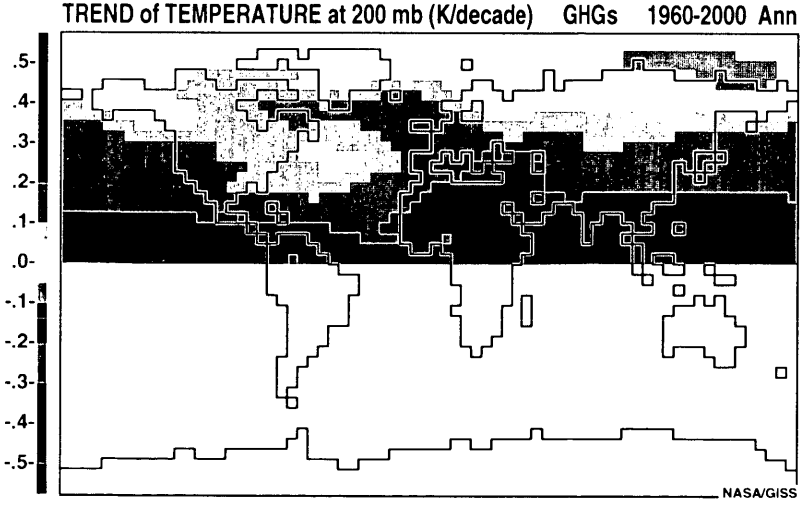
TREND of TEMPERATURE at 200 mb (K/decade) GHGs 1960-2000 Ann
.5-
.4-
.3-
.2-
.1-
.0-
-.1-
-.2-
-.3-
-.4-
-.5-
NASA/GISS

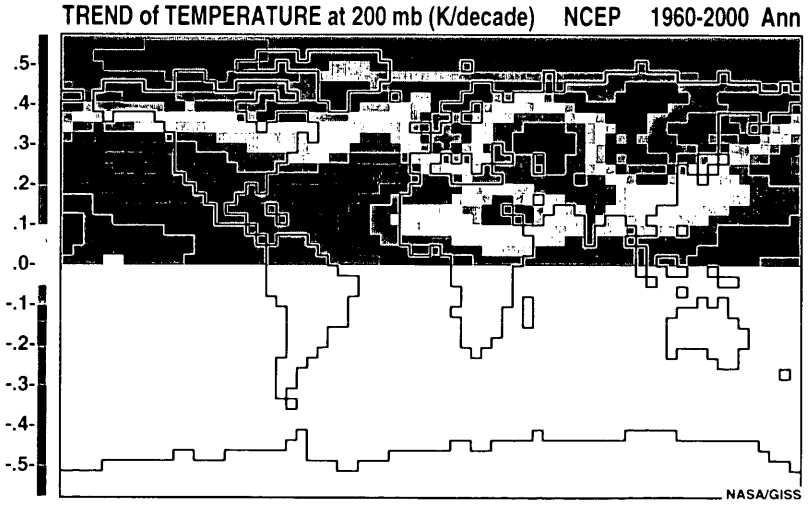
TREND of TEMPERATURE at 200 mb (K/decade) NCEP 1960-2000 Ann
.5-
.4-
.3-
.2-
.1-
.0-
-.1-
-.2-
-.3-
-.4-
-.5-
NASA/GISS

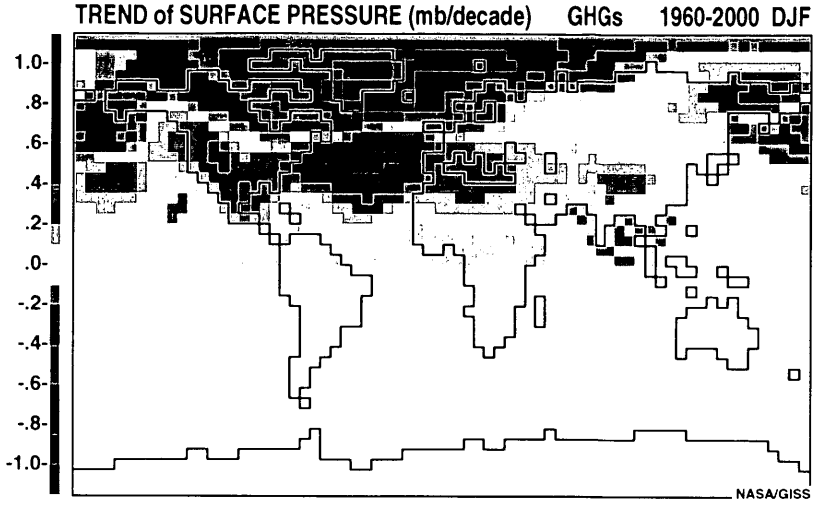
TREND of SURFACE PRESSURE (mb/decade) GHGs 1960-2000 DJF
1.0
.8
.6
.4
.2
.0
-.2
-.4
-.6
-.8
-1.0
NASA/GISS

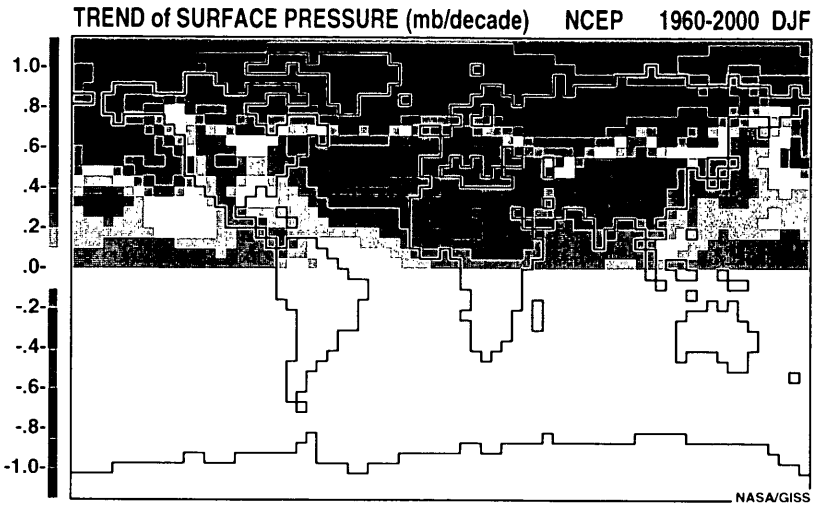
TREND of SURFACE PRESSURE (mb/decade) NCEP 1960-2000 DJF
1.0
.8
.6
.4
.2
.0
-.2
-.4
-.6
-.8
-1.0
NASA/GISS

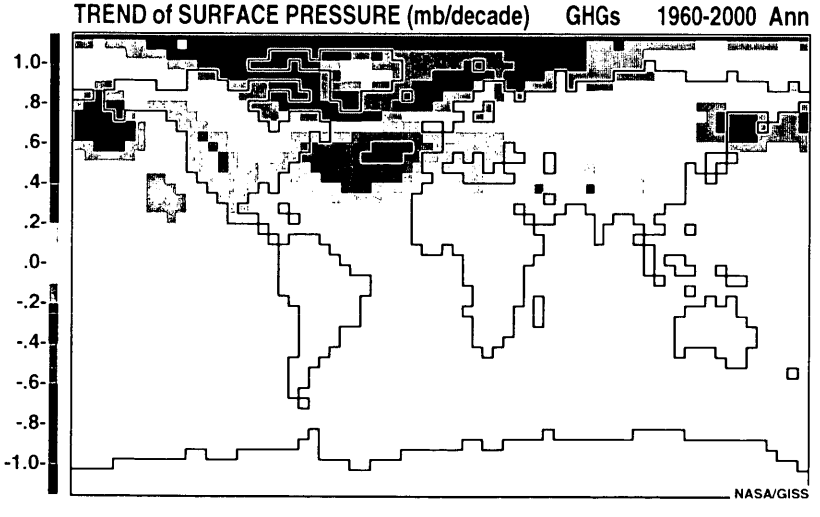
TREND of SURFACE PRESSURE (mb/decade) GHGs 1960-2000 Ann
1.0
.8
.6
.4
.2
.0
-.2
-.4
-.6
-.8
-1.0
NASA/GISS

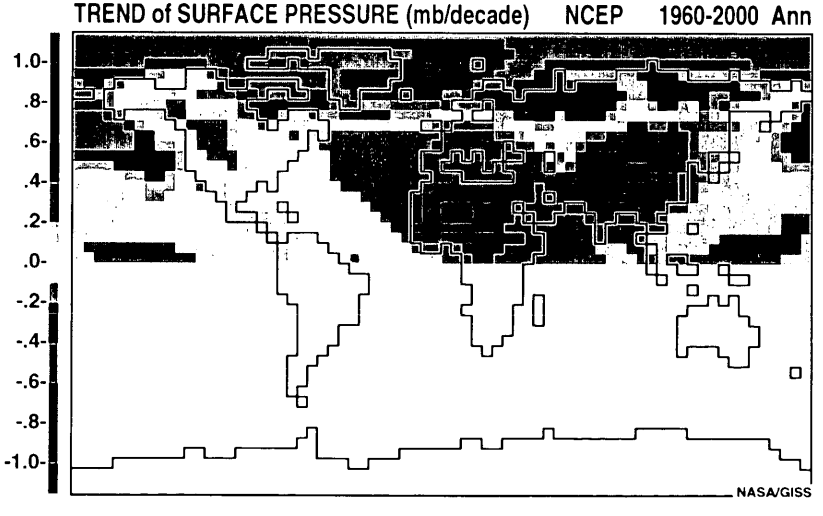
TREND of SURFACE PRESSURE (mb/decade) NCEP 1960-2000 Ann
1.0
.8
.6
.4
.2
.0
-.2
-.4
-.6
-.8
-1.0
NASA/GISS

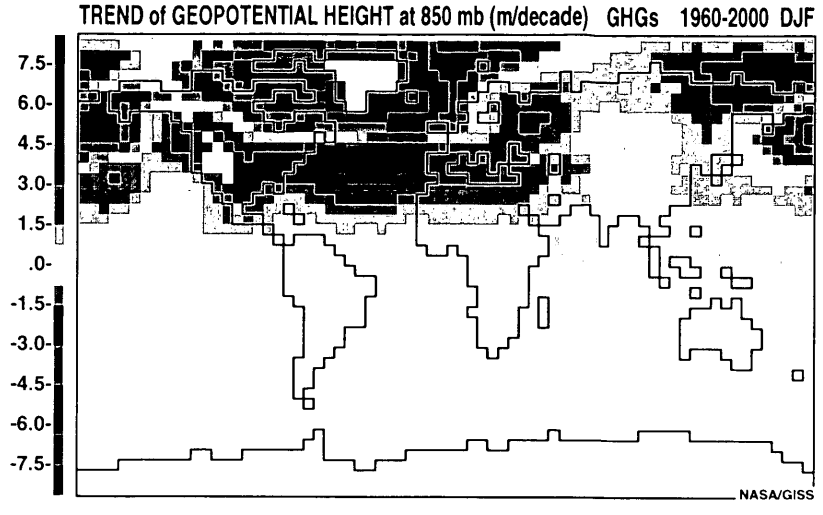
TREND of GEOPOTENTIAL HEIGHT at 850 mb (m/decade) GHGs 1960-2000 DJF
7.5
6.0
4.5
3.0
1.5
.0
-1.5
-3.0
-4.5
-6.0
-7.5
NASA/GISS

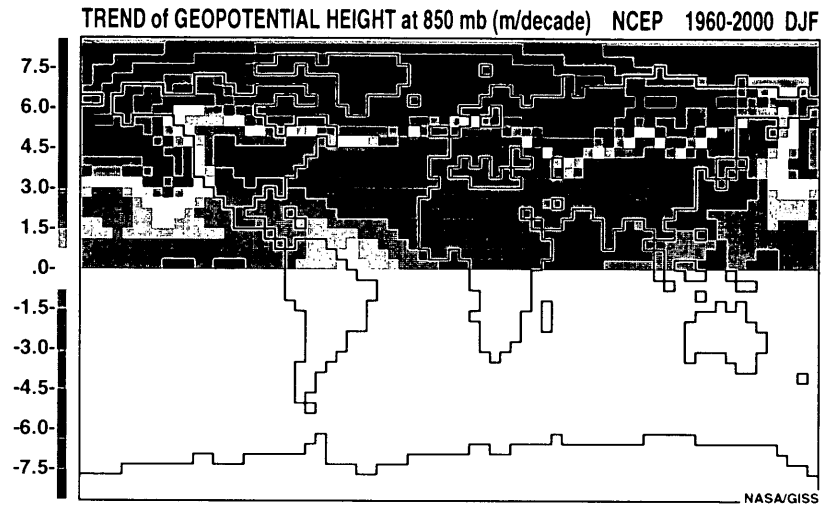
TREND of GEOPOTENTIAL HEIGHT at 850 mb (m/decade) NCEP 1960-2000 DJF
7.5
6.0
4.5
3.0
1.5
.0
-1.5
-3.0
-4.5
-6.0
-7.5
NASA/GISS

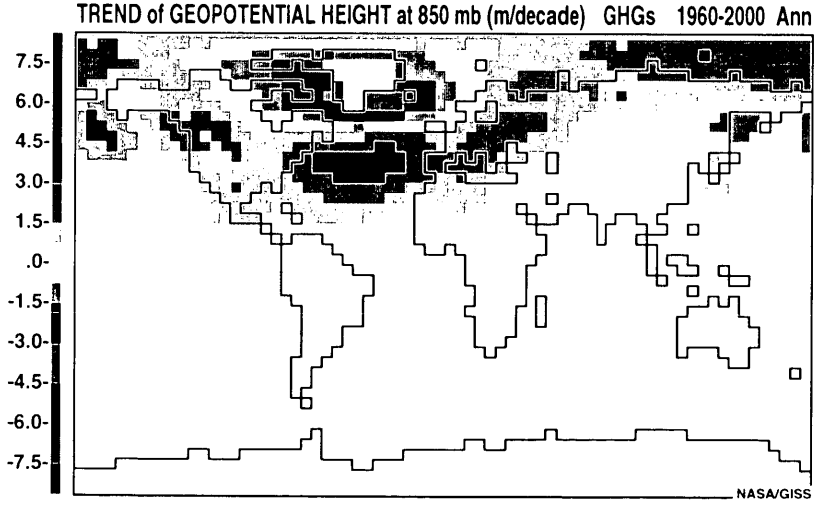
TREND of GEOPOTENTIAL HEIGHT at 850 mb (m/decade) GHGs 1960-2000 Ann
7.5
6.0
4.5
3.0
1.5
.0
-1.5
-3.0
-4.5
-6.0
-7.5
NASA/GISS

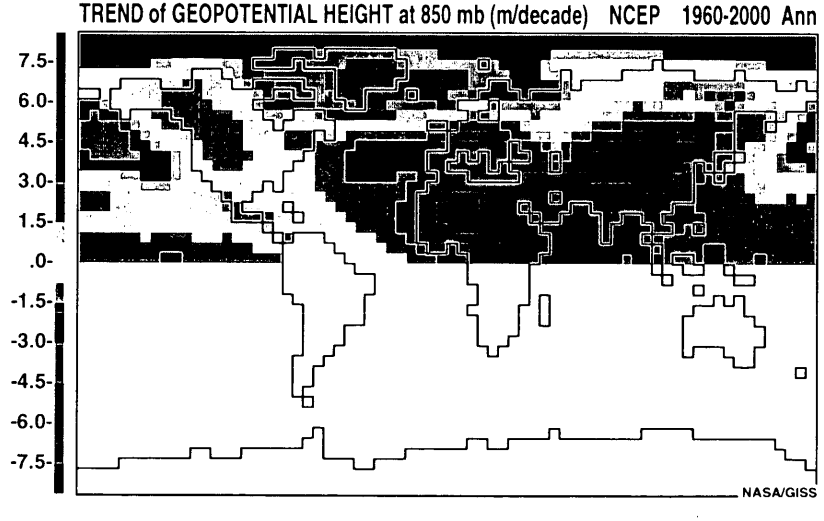
TREND of GEOPOTENTIAL HEIGHT at 850 mb (m/decade) NCEP 1960-2000 Ann
7.5
6.0
4.5
3.0
1.5
.0
-1.5
-3.0
-4.5
-6.0
-7.5
NASA/GISS

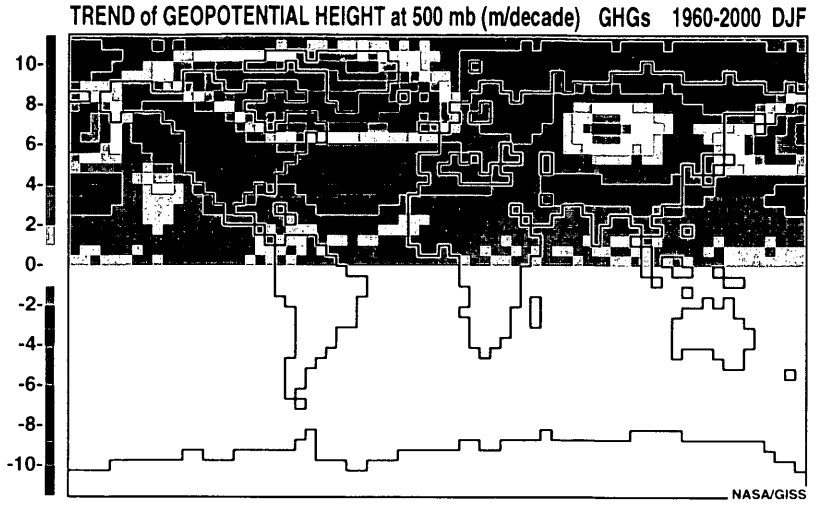
TREND of GEOPOTENTIAL HEIGHT at 500 mb (m/decade) GHGs 1960-2000 DJF
10-
8-
6-
4-
2-
0-
-2-
-4-
-6-
-8-
-10-
NASA/GISS

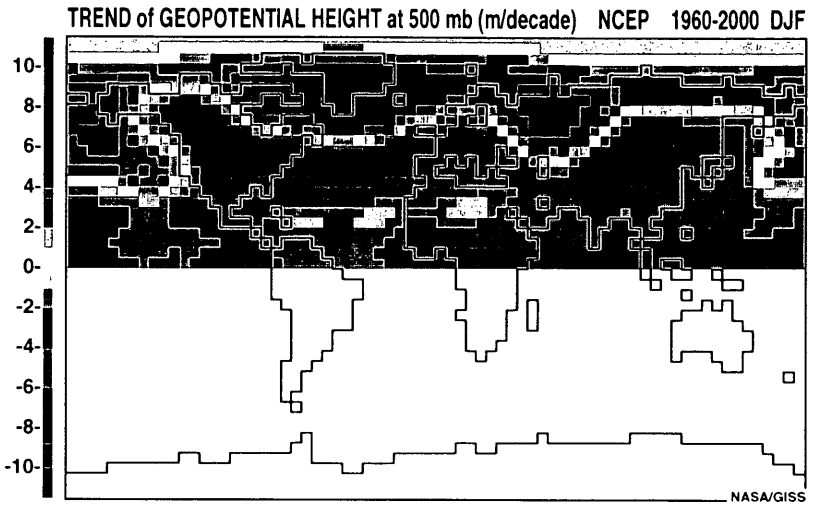
TREND of GEOPOTENTIAL HEIGHT at 500 mb (m/decade) NCEP 1960-2000 DJF
10-
8-
6-
4-
2-
0-
-2-
-4-
-6-
-8-
-10-
NASA/GISS

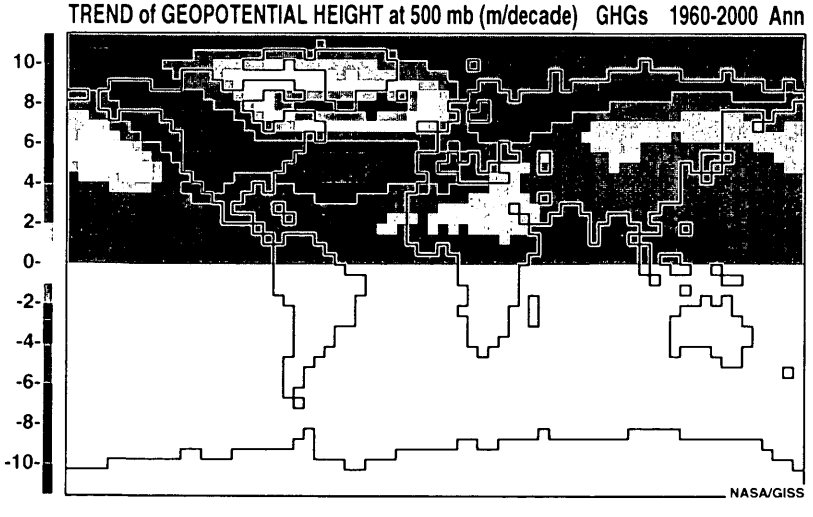
TREND of GEOPOTENTIAL HEIGHT at 500 mb (m/decade) GHGs 1960-2000 Ann
10-
8-
6-
4-
2-
0-
-2-
-4-
-6-
-8-
-10-
NASA/GISS

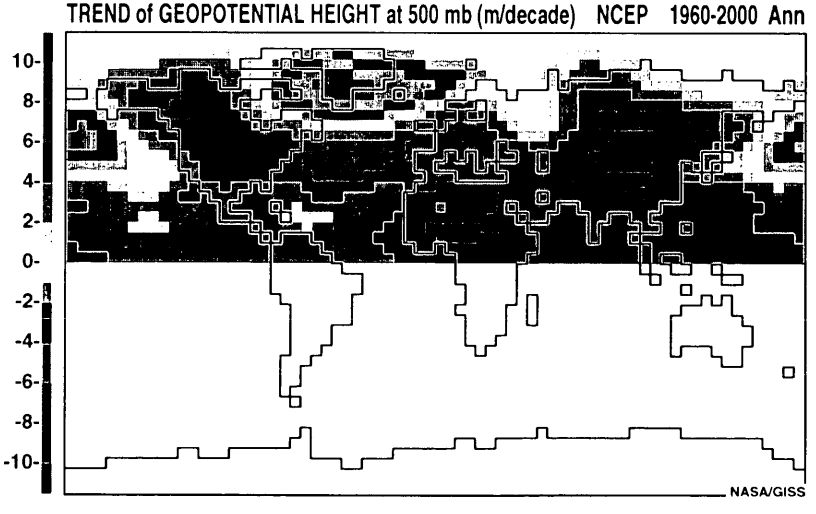
TREND of GEOPOTENTIAL HEIGHT at 500 mb (m/decade) NCEP 1960-2000 Ann
10-
8-
6-
4-
2-
0-
-2-
-4-
-6-
-8-
-10-
NASA/GISS

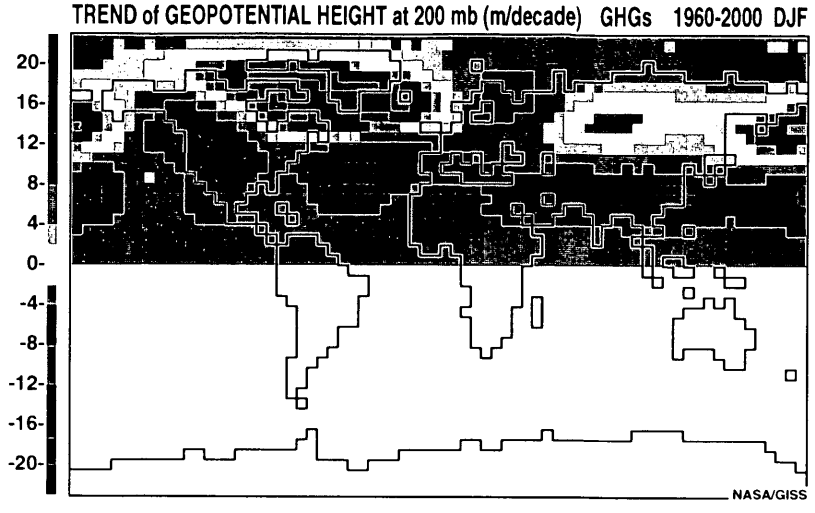
TREND of GEOPOTENTIAL HEIGHT at 200 mb (m/decade) GHGs 1960-2000 DJF
20-
16-
12-
8-
4-
0-
-4-
-8-
-12-
-16-
-20-
NASA/GISS

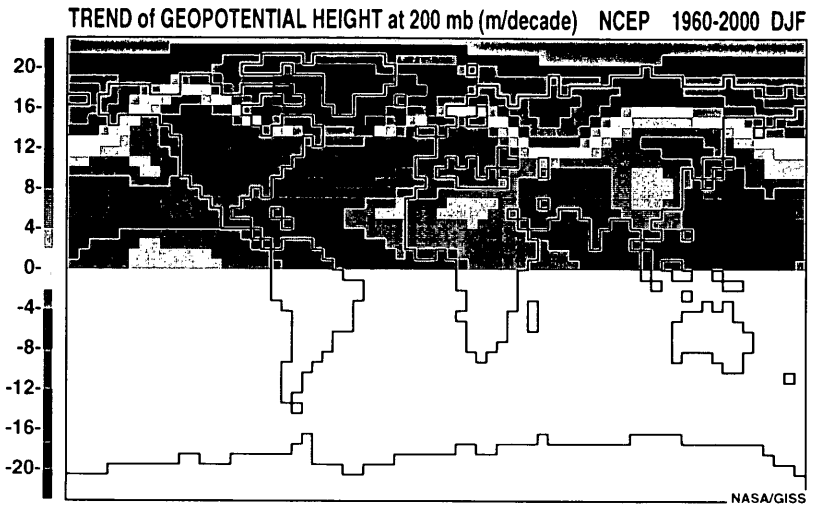
TREND of GEOPOTENTIAL HEIGHT at 200 mb (m/decade) NCEP 1960-2000 DJF
20-
16-
12-
8-
4-
0-
-4-
-8-
-12-
-16-
-20-
NASA/GISS

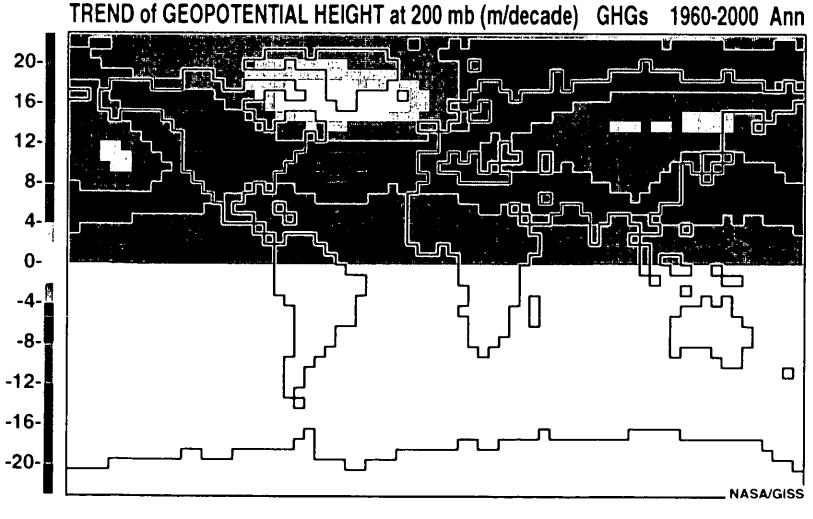
TREND of GEOPOTENTIAL HEIGHT at 200 mb (m/decade) GHGs 1960-2000 Ann
20-
16-
12-
8-
4-
0-
-4-
-8-
-12-
-16-
-20-
NASA/GISS

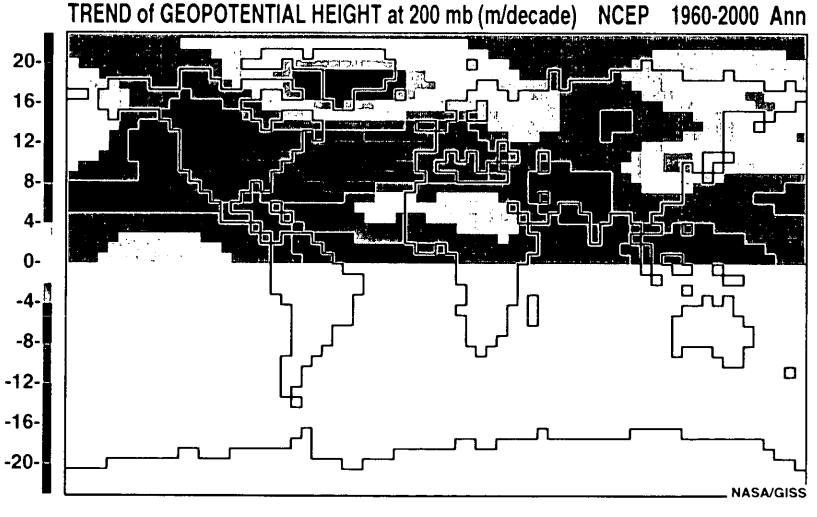
TREND of GEOPOTENTIAL HEIGHT at 200 mb (m/decade) NCEP 1960-2000 Ann
20-
16-
12-
8-
4-
0-
-4-
-8-
-12-
-16-
-20-
NASA/GISS